

^{152/154}Eu(III) Ions Sorption on Stannic Silicate Granules: A Radiotracer Study

I. M. ALI*, H. A. MADBOULY and M. M. EL-SHORBAGY

Hot Labs Centre, Atomic Energy Authority, P.C. 13759, Cairo, Egypt
ismail-m_ali@yahoo.com

Received 16 October 2018 / Accepted 20 November 2018

Abstract: Silicates and related porous materials are solids able to interact with guest molecules, ions and atoms not only at their surfaces but also within the bulk. With the objective of producing materials showing better sorption properties, a laboratory prepared stannic silicate in mixed SnO₂@SiO₂ form was investigated as potential sorbent for retention of long lived radionuclides ¹⁵²⁺¹⁵⁴Eu³⁺ from aqueous solution containing ¹³⁴Cs⁺ and ⁶⁰Co²⁺. Sorption of Eu³⁺ has been reported as a function of contact time, initial ion concentration and temperature at a constant pH equal to 4. The uptake of Eu³⁺ was found to be favored at high ion concentration, high temperature and no significant sorption took place after the first 4 h. A pseudo second order kinetic pattern fitted the sorption data well, while equilibrium was positively verified with Freundlich-type equation. Further, in attempt to enhance the separation efficiency of the studied radionuclides from aqueous medium, results showed that the sorption on SnSi was found strongly temperature-dependent. Ions equilibrium was found exothermic in case of ¹³⁴Cs⁺ however it endothermic in case of both ⁶⁰Co and ¹³⁴Cs ions. Based on this contradict uptake, selectivity of ions has been estimated and separation of Eu³⁺ from other competing ions was achieved. The thermodynamic parameters (ΔG° , ΔH° and ΔS°) showed that the adsorption process is spontaneous and exothermic in case of ¹³⁴Cs⁺ but it endothermic in case of the later studied ions.

Keywords: Stannic silicate, Radiotracer, Removal, Kinetic studies, Sorption isotherm

Introduction

Due to rapid population growth, technological advancement and nuclear activities the rate of generated waste effluents has become a grave concern. These effluents are dangerous to human health and environment and have stimulated a renewed interest in monitoring, control and removal^{1,2}. In reprocessing of nuclear spent fuel, many kinds of radionuclides such as uranium, europium, strontium, cesium and many other transuranic elements and fission products are of high toxicity, long half-life and carcinogenicity. Among these radionuclides, trace level concentration of radio-europium (¹⁵²⁺¹⁵⁴Eu³⁺) which possesses high fission yield is generally transferred to liquid wastes. As a result, the removal or separation of such nuclides from wastewater is imperative from the health point of view. However the

$^{134}\text{Cs}^+$ and $^{60}\text{Co}^{2+}$ isotopes are commonly present in radioactive wastes beside $^{152+154}\text{Eu}^{3+}$ and owing to their relatively long half-lives (2.06, 5.27, 8.59 and 13.54y for $^{134}\text{Cs}^+$, $^{60}\text{Co}^{2+}$, $^{154}\text{Eu}^{3+}$ and $^{152}\text{Eu}^{3+}$, respectively) as well as their radio-toxicity, these nuclides must be removed from wastes for safe discharge^{3,4}. Europium as one metal belongs to the REEs is only stable in Eu^{3+} in aqueous solution and has used mainly in the manufacture of cathode ray tubes, fluorescent lamp and screen for x-rays. In nuclear industry europium has used as neutrons absorbent for the extinction and control rods of the reactors. Efficient separation of trace concentration fission products and other spent fuel constituents is necessary to enable various disposals or recycle options. Thus, the study of sorption kinetics in wastewater treatment is important in providing valuable insights into the reaction pathways and into the mechanism of adsorption reaction. Recently, adsorption as process for treating contaminated water has been object of several investigations because this method allows removal of a great amount of water polluting agents on several types of adsorbent materials; moreover, this method has shown to be economic and highly effective⁵. Adsorption can be defined as the accumulation of ions at the solid-liquid interface due to different types of forces. The sorption of $^{152+154}\text{Eu}(\text{III})$ on clay minerals, metal oxides and nanomaterials had been extensively studied in the last decade⁶⁻¹¹. The results suggested that the sorption of $\text{Eu}(\text{III})$ was strongly dependent on ionic strength and pH ⁶⁻¹¹. The sorption was mainly dominated by outer-sphere surface complexation and/or ion exchange at low pH , and by inner-sphere surface complexation and/or surface co precipitation at high pH values⁶⁻¹¹. The removal of radioactive europium from nuclear waste solutions is important from the point of view of their toxicity and therefore has been of interest^{12,13}. Among various types of inorganic ion exchangers available, silicates appears to be quite promising in the treatment of low- and high-level radioactive wastes¹⁴⁻¹⁷. Silicates have been reported to be important ion exchange materials as they are irradiation and temperature resistant¹⁴⁻¹⁶. The ion exchange properties of the H^+ form of crystalline stannic silicate, referred to as H-CSi indicate high ion selectivity^{12,13,18} for $^{152+154}\text{Eu}^{3+}$. Adsorption isotherms developed from theoretical and/or empirical considerations are used to quantify such processes. This can be made by relating the solute concentration on liquid and solid phase at equilibrium condition. There are also many kinds of oxygen-containing functional groups such as Fe-OH , Al-OH , Si-OH and $-\text{OH}$ groups on silicate surfaces, which can form strong surface complexes with metal ions and thereby can remove heavy metal ions from aqueous solutions efficiently. Fan *et al*^{19,20}, studied sorption of $\text{Ni}(\text{II})$ and $^{152+154}\text{Eu}(\text{III})$ on humic acid-bound attapulgite and found that humic acid could act as a "bridge" between metal ions and attapulgite. Ali *et al.*, reported the synthesis and sorption mechanism of ^{22}Na , ^{134}Cs and ^{60}Co on stannic silicate(SnSi)²¹.

In this paper, we evaluated the sorption behaviour of $^{152+154}\text{Eu}^{3+}$ from aqueous nitrate solution onto SnSi granules as a function of concentration, time and temperature using radiotracer technique. Kinetic, sorption isotherm, thermodynamic and selectivity of Eu^{3+} have been analyzed and discussed.

Experimental

All chemicals used were of analytical grade purity (A.R. Grade).

Synthesis and characterization of SnSi

The synthesis of SnSi granules was based on the wet chemical precipitation procedure as described previously by our group²¹. In a typical preparation, equal volumes of equimolar ratios (0.1 M) each of SnCl_4 and Na_2SiO_3 were mixed in drop wise addition at room temperature. The precipitation pH was adjusted by ammonia solution. The formed precipitation

of white gel had settled, for 48 h in mother liquor. Discard of the suspended material and separation of the settled portion, the precipitated gel was washed three times by shaking thoroughly with deionized water. It was then filtered off and dried in an automatic oven at 60 °C. Part of the product was converted to H^+ form (acid modified) by treating with 1 M nitric acid, then washed carefully by double distilled water and re-dried at 60 °C. The products were ground and sieved to give the suitable mesh size of 225-425 μm . The prepared samples were air dried and stored at the ambient room temperature.

X-ray, IR, thermal and elemental analyses

Powder x-ray diffraction (XRD) was performed using a Shimadzu x-ray diffractometer; model XD 610, with a nickel filter and K_{α} Cu radiation ($1.54^{\circ}A$) operating at 30 kV and 30 mA. Thermal analysis was determined using a Shimadzu DT-60 thermal analyzer obtained from Shimadzu, Kyoto "Japan". The samples measured for ambient temperature up to 1000 °C with a heating rate of 15 deg /min under nitrogen atmosphere. The FTIR spectra were acquired with a Bomem FTIR spectrometer applying KBr disc technique. The x-ray fluorescence was carried out using Phillips x-ray fluorescence model PW 2400 spectrometer by applying the pressed technique.

Adsorbate

The solutions containing 10^{-6} - 10^{-4} M each of Eu^{3+} were prepared by dissolving a weighed quantity of $Eu(NO_3)_3$ in deionized water. Carrier free $^{152+154}Eu^{3+}$ in a similar chemical forms were subsequently used to label the solutions. The initial pH of each solution was adjusted to the required value (pH =4) by adding HNO_3 solution. It should be noted that nitrate anions are not forming precipitates or complexes at the test conditions and are considered to be inert. The progress of adsorption radionuclides was measured by, placing of 0.05 g of SnSi in 5 mL of the corresponding labeled aqueous solutions of desired concentrations and pH, stirring at regular intervals and equilibrating. The supernatant solutions withdrawn before and after addition of solid adsorbent were assayed for their γ -activity.

Radioactive materials

The radioactive tracer $^{152+154}Eu^{3+}$ isotopes were locally prepared. In this respect, highly pure spectroscopic $Eu(NO_3)_3$ was used as target and warped in an aluminum can and irradiated with neutrons for 48 hours in the Egyptian 2 MW research reactor at inshas, using a neutron flux of $1.3 \times 10^{13} n.cm^{-2}.s^{-1}$. The obtained radionuclides were dissolved and diluted with double distilled water and were used as tracers in the equilibrium measurements.

Radioactive assay

The radioactive nuclides used in the present work were assayed by measuring the γ -activity of $^{152+154}Eu^{3+}$ using a scintillation detector head (NaI) connected to scalar of the type SR-7 obtained by nuclear enterprises, USA. In most cases the counting rates were at least ten times greater than of the background. Each result recorded in this work, tabulated or graphed is a mean value of three readings obtained under the same geometrical conditions and calculated after correction for background.

Sorption studies

The removal percentage for the present adsorption processes onto SnSi was calculated using the following equation:

$$\text{Removal \%} = (A_i - A_f) / A_i \times 100 \quad (1)$$

Where A_i and A_f are the initial and final radioactivity of radionuclide, respectively. The amounts of Eu(III) ions adsorbed per gram of SnSi (q , meq/g) at a specific contact time (q_t) or at equilibrium (q_e) were determined by the following equation:

$$q_t \text{ or } q_e = \text{Removal \%} / 100 \times V/m \times C_o \quad (2)$$

Where C_o is the initial concentration of the adsorbate (M), V is the volume of the adsorbate solution (L) and m is the weight of SnSi (g). The distribution ratio (K_d) was calculated from the following equation:

$$K_d = (A_i - A_e / A_e) \cdot V/m \quad (\text{mLg}^{-1}) \quad (3)$$

Where A_i and A_e represent the radioactivity of the initial and equilibrium aliquots withdrawn, respectively. V is the volume of adsorbate (mL) and m is the mass of adsorbent (g).

Selective sorption studies

The selectivity of SnSi for Eu ions over other metal ions were evaluated from the selectivity coefficient ($K_{\text{Eu}^{3+}/\text{M}^{n+}}$), which was determined by incubating 0.05 g of granules with each individual selected metal ions present in 5 mL of DDW under identical conditions. The selectivity coefficient $K_{\text{Eu}^{3+}/\text{M}^{n+}}$ is defined as^{21,22}:

$$K_{\text{Eu}^{3+}/\text{M}^{n+}} = K_a = K_d(\text{Eu}^{3+}) / K_d(\text{M}^{n+}) \quad (4)$$

K_a is the separation factor provides a guideline for metal separation. The greater the deviation of K_a from unity better is the separation.

Where $K_d(\text{Eu}^{3+})$ and $K_d(\text{M}^{n+})$ are the distribution ratios of Eu(III) ions and other coexistent metal ions (Cs^+ and Co^{2+}), respectively.

All the experiments were conducted in triplicate and average values were used in the data analysis and the results agreed to $\pm 3\%$.

Results and Discussion

With the objective of producing a material showing better sorption properties to be used for treatment of spent fuel species, SnSi in granule nature was prepared. The procedure for preparation is described previously²¹. Our approach to improving the structural stability is to incorporate a tin compound into a SiO_2 matrix, which is structurally stable and hence offers structural stability to the radioactive waste management. The proposed $\text{SnO}_2\text{-SiO}_2$ structure will facilitate the penetration of the radionuclide into the sorbent surface and hence increase the rate of ion exchange. As reported in our previous work²¹, SnSi was found to be chemically and thermally stable among the Sn(IV) inorganic ion exchangers and it was found possess ion exchange capacity 0.96 meq/g for Cs^+ .

Material characterization

X-ray, thermal and IR studies

According to crystal diffraction analysis (Figure 1) for SnSi (H^+ -form) samples heated at 50, 600 and 1000 °C, an amorphous structure with no change after heating up to 600 °C was appeared. After heating at 1000 °C, 3 major peaks with maxima at 26.9, 34.2 and 52.12° corresponding to lattice planes (hkl) 110, 101 and 211 were recorded, respectively. The obtained peaks were comparable to the SnO_2 , JPCDS 1983 card no: 41-1445 data²². All of the observed peaks in the XRD pattern in Figure 1, are indexed assuming SnO_2 cassiterite phase, giving all peaks positions, the non-existence of any other overlapping peak in the standard peak positions indicates that the SnO_2 in the prepared sample has a single phase, *i.e.* the existence of only SnO_2 molecules. It is further observed that there is no indication of

the presence of SiO_2 peaks. This confirms that only in this obtained Sn/Si system the SnO_2 apple to crystallize while the SiO_2 still present in randomly arranged nature. In addition, this result evidences that the direct chemical interaction of SnO_2 with SiO_2 does not occur in the composite. Similar behavior was reported for $\text{SiO}_2/\text{SnO}_2$ mixed oxides obtained by the sol-gel process at high temperature²³. Also, L. Kurihara²⁴ indicated that no peaks assignable to the SiO_2 crystalline phase are observed in case of $\text{SiO}_2/\text{SnO}_2$ obtained by the sol-gel processing method after heating up to 1473 K. Infrared analysis confirmed the purity of the stannic silicate, whose characteristic absorption and observed in the spectrum (Figure 2) were as follows: at 3200-3500 cm^{-1} is due to the stretching vibration of water molecules, while the sharp peak at 1635 cm^{-1} is due to the bending vibration of H_2O molecules. The shoulder at 3246 cm^{-1} could be assigned to the stretching vibrations of Si-OH groups in the structure of amorphous SiO_2 . The peak at 1040 is characteristic of $\nu\text{Si-O}$ of SiOH (silanol) group while the peak at 960 cm^{-1} is associated with Si-O-Sn vibration²⁵. High decreases in all intensities of molecular water peaks were reported when samples heated at 600 and 1000 $^\circ\text{C}$ (dehydration process).

The DT/TGA thermogram of SnSi was depicted in Figure 3. The figure shows a total weight loss of about 22.25% for sample heated up to 1000 $^\circ\text{C}$. Above 500 $^\circ\text{C}$, there are no any thermal changes and the weight remained constant. In parallel, the DTA curve shows an endothermic peak with maximum at 80 $^\circ\text{C}$ corresponding to dehydration of 16.4% of water molecules corresponding to the physical adsorbed water and structural water. The latter change (5.85%) may arise from SiOH and SnOH polycondensation²⁴.

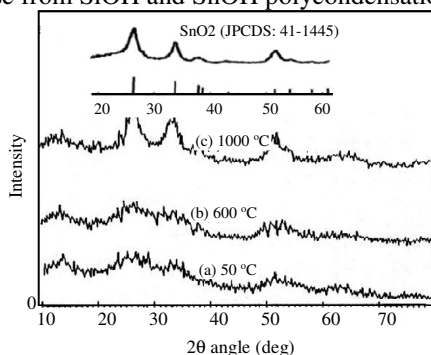


Figure 1. XRD patterns of SnSi preheated at different temperature

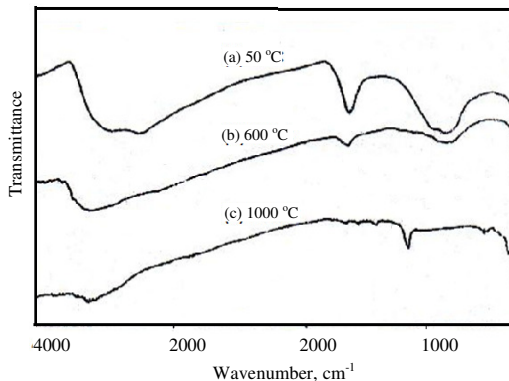


Figure 2. IR spectra of SnSi preheated at different temperature

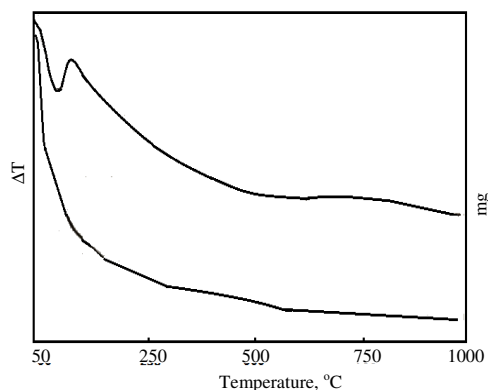


Figure 3. DTA/TG thermogram of SnSi

Time dependent adsorption

According to the speciation curve of europium, Eu^{3+} (+3 oxidation state) is the main stable species till $\text{pH} < 6$ and $\text{Eu}(\text{OH})_3$ species is the major form exists at $\text{pH} > 6$ ^{8,26,27}. In this work, pH 4 was selected for sorption of $\text{Eu}(\text{III})$ ions over the surface of SnSi (H-form) as a function of contact time at concentration range 10^{-6} - 10^{-4} M. As shown in Figure 4, a sharp initial rise of sorption attaining an apparent saturation within 240 min of contact time at all concentrations was obtained. No further change in sorption is observed even after a contact time of 24 h. In the initial stage of the sorption process, the surface coverage is too low that cause increasing driving force to overcome the resistance to mass transfer of radionuclides from the aqueous phase to the solid phase. However with the lapse of time as the blocking of active sites increase, the rate of uptake becomes slower and an apparent equilibrium stage is reached. The amount adsorbed at equilibrium increased from 0.84×10^{-4} (28% uptake) to 0.48×10^{-2} (16% uptake) mol g^{-1} with increasing adsorptive concentration of radio activities metal ion from 10^{-6} to 10^{-4} M. The relative increase of uptake with the dilution suggests that chemi-complexation occurring on SnSi surface. This change is applicable in the light of fact that, more and more surface sites are available for deposition of a relatively smaller number of $\text{Eu}(\text{III})$ ions at higher dilution. In parallel, the rate of uptake becomes slower with oncoming to the equilibrium. This is due to increase of blocking of active sites of adsorbent and saturation of the available sorption sites with increasing radioactivity.

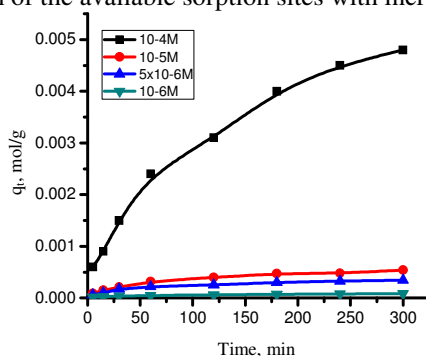


Figure 4. Time variation of $\text{Eu}(\text{III})$ ions on SnSi at various concentrations of adsorptive solution and at 25 ± 1 °C

Adsorption kinetics

The adsorption kinetics, which depends deeply on the physical and/or chemical characteristics of the adsorbent, describes the reaction pathways and reaction rates. To investigate the kinetic parameters for Eu(III) adsorption by SnSi at room temperature, the data were analyzed by means of the following models; pseudo-first-order and pseudo-second-order models (Eqs. 5 and 6). The two models were used to predicate the sorption mechanism. Comparing the correlation coefficients (R^2) values yielded from the two models for sorption process it can be determine the more obeyed mechanism.

The simple linearized forms of these equations are expressed as Dolatyari *et al.*,²⁸ and Duman *et al.*,²⁹:

For first order;

$$\log (q_e - q_t) = \log q_e - (k_1 / 2.303) t \quad (5)$$

For second order;

$$t/q_t = 1 / K_2 q_e^2 + t/q_e \quad (6)$$

Where q_e and q_t are the amounts of Eu^{3+} adsorbed (mol g^{-1}) at equilibrium and time t (min), respectively, and k_1 ($1/\text{min}$) and k_2 ($\text{g mol}^{-1} \text{min}^{-1}$) are the adsorption rates for the pseudo-first-order and pseudo-second-order adsorptions, respectively. Rate constants, k_1 is calculated from the slopes of the linear plots of $\log (q_e - q_t)$ vs. t (Eq. 5), while k_2 is calculated from the intercepts of the linear plots of t/q_t versus t (Eq. 6). From the slope and intercept values of linear fittings of the experimental kinetics of $^{152+154}\text{Eu}^{3+}$ onto SnSi to the aforementioned kinetic models (Figures 5, 6), the kinetic parameters are calculated and the data obtained are tabulated in Table 1.

Table 1. Kinetic parameters of Eu^{3+} sorption on SnSi at different concentrations and at pH =4

C_0, M	$q_{e, \text{exp}}, \text{meq g}^{-1}$	Pseudo-first-order model			Pseudo-second-order model			Elovich model			
		K_1, min^{-1}	$q_e, \text{meq g}^{-1}$	R^2	$K_2, \text{g mol}^{-1} \text{min}^{-1}$	$q_e, \text{meq g}^{-1}$	R^2	β	∞	R^2	$h = K_2 q_e^2$
10^{-4}	0.0048	0.0104	0.00024	0.97	0.047	0.00028	0.97	900.91	2.13×10^{-4}	0.97	1.3×10^{-5}
10^{-5}	0.00054	0.009	0.00021	0.96	0.888	0.000028	0.99	8781.9	3.47×10^{-5}	0.94	2.5×10^{-5}
5×10^{-6}	0.000345	0.011	0.000012	0.89	1.434	0.0000186	0.98	13944.5	2.57×10^{-5}	0.98	2.7×10^{-5}
10^{-6}	0.000084	0.0092	0.000003	0.97	68.03	0.0000013	0.98	60496.1	6.87×10^{-6}	0.97	8.8×10^{-5}

In this study, the initial concentration of Eu(III) is determined as 10^{-6} - 10^{-4} M. From Table 1, when comparing the correlation coefficients (R^2) obtained at different concentrations for two models, it was found that the R^2 obtained from the pseudo-second-order model are higher (larger than 0.98 for all concentrations) than their fittings to the pseudo-first-order model. Also, the estimated values of q_e calculated from the equation of pseudo-second-order model is more comparable with the experimental values ($q_{e, \text{exp}}$). Therefore, the adsorption reaction can be approximated more favorably by the pseudo-second-order. This model based on the assumption that, the rate-determining step may be a chemical sorption involving valence forces through sharing or exchange of electrons between the adsorbent and the adsorbate³⁰. Accordingly, adsorption may involve sharing of electrons between Eu(III) ions and SnSi³⁰. Moreover, using the calculated pseudo-second-order rate constants and adsorption capacities ($q_{e(\text{cal})}$), the initial sorption rate (h) can be determined using eq. 7 and listed in Table 1.

$$h = K_2 q_e^2 \quad (7)$$

The tabulated initial sorption rate values indicated that they decreased with enhancing the initial ions concentration.

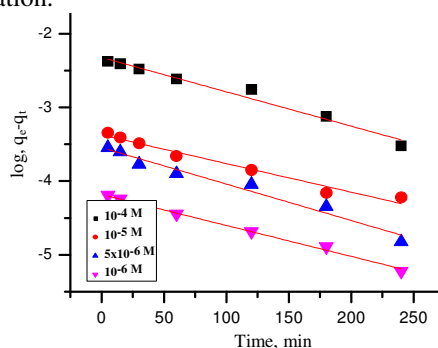


Figure 5. Plot of $\log (q_e - q_t)$ with time for sorption of Eu^{3+} on SnSi

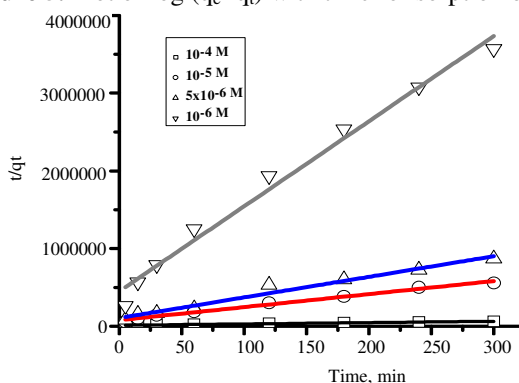


Figure 6. Plot of t/q_t with time for sorption of Eu^{3+} on SnSi

Elovich model

This model is generally expressed as follows³¹:

$$dq_t/dt = \alpha \exp(-\beta q_t) \quad (8)$$

Where α is the initial Eu^{3+} sorption rate [mmol/(g min)] and β is the desorption constant (g/mmol) during any one experiment. To simplify the Elovich equation, Chien and Clayton (1980) assumed $\alpha \beta t \gg 1$ and on applying the boundary conditions $q_t = 0$ at $t = 0$ and $q_t = q_t$ at $t = t$, equation (8) then becomes³²:

$$q_t = \alpha + \beta \ln t \quad (9)$$

Equation 9 was used to test the applicability of the Elovich equation to the kinetics of Eu^{3+} sorption on to SnSi. The plot of q_t vs. $\ln t$ should give a linear relationship for the applicability of the simple Elovich kinetic (Figure 7). The constants β and α could be estimated from the slope and intercept of the linearization of the simple equation (Table 1). Table 1 declared that the Elovich equation also fit with the experimental data well with high correlation coefficients.

Sorption isotherm

Sorption isotherms are generally used to determine the sorption capacity of an adsorbent. In the present study, the partition of Eu^{3+} at equilibrium between liquid and solid phases was

modeled using the adsorption isotherms of Langmuir and Freundlich. The equations of these isotherms are, respectively, given by:

$$C_e/q_e = C_{eq}/q_{max} + 1/b q_{max} \quad (10)$$

$$\log q_e = 1/n \log C_{eq} + \log K_F \quad (11)$$

where, C_e (mol/L), q_e (meq/g), q_m (meq/g) and b are the Eu^{3+} equilibrium concentration (mol/L), equilibrium adsorption capacity (meq/g), maximum adsorption capacity (meq/g), and Langmuir constant (L mg^{-1}), respectively. Besides, K_F and n are the Freundlich constants (system specific constants) which indicate the adsorption capacity and a constant indicating the adsorption intensity, respectively. The two isotherm models were checked by plotting C_e/q_e against C_e (Figure 8a) and $\ln q_e$ versus $\ln C_e$ (Figure 8b). The corresponding constants for each model were estimated from the slope and intercept of the relevant straight line and they were tabulated in Table 2. The maximum adsorption capacity ($q_{m(\text{cal})}$) of SnSi calculated from the Langmuir model was found to be 0.128 meq/g which is too far with the experimentally obtained.

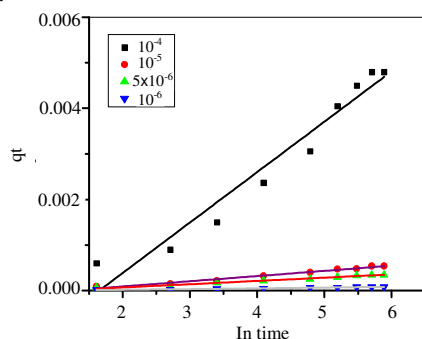


Figure 7. Plot of q_t against $\ln t$ for the sorption of Eu^{3+} on SnSi

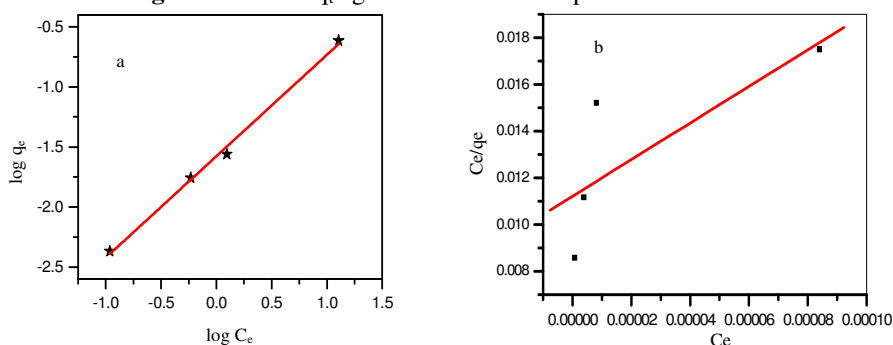


Figure 8. Freundlich(a) and Langmuir (b) sorption isotherms of europium ions on SnSi at 25 °C

On the other hand, the maximum sorption capacity ($q_{m(\text{cal})}$) utilizing the Freundlich isotherm was estimated to be 6.6×10^{-4} meq/g. Comparison between the tabulated constants in Table 2 for both applied isotherm models exhibited that sorption of Eu^{3+} on SnSi followed the Freundlich model.

The statistical theory of adsorption³³ reported that the isotherms with $0 < 1/n < 1$ are attributed to a heterogeneous structure of the surface without any interactions between adsorbed atoms or molecules. In the present investigation a somewhat higher value of

$1/n(0.845)$ clearly corresponds to a heterogeneous surface with an exponential distribution of energy of the adsorption sites³⁴. A relatively high value of $K_F(1.58)$ further confirms a higher affinity of Eu(III) for SnSi. This value of K_F are in the same order of magnitude of the value obtained for the normal type adsorption system of Eu(III) ion on hydroxyapatite³⁵.

Table 2. The parameters of Langmuir and Freundlich isotherms simulation of Eu(III) sorption on SnSi

Isothermmodel	Parameter	Value
Langmuir	$b \text{ (L mg}^{-1}\text{)}$	72.0
	$q_{m(\text{cal})}$	0.128 (meq/g)
	R^2	0.41
	$q_{e(\text{exp})}$ at $C_0=10^{-4} \text{ M}$	8.4×10^{-5} (meq/g)
Freundlich	$K_F[(\text{mg g}^{-1}) (\text{L mg g}^{-1})^{1/n}]$	-1.58
	$q_{m(\text{cal})}$	6.6×10^{-4} (meq/g)
	R^2	0.99
	n	0.845

Sorption capacity

Actual radioactive wastewater and/or the spent fuel usually contain a variety of metal ions. Low selectivity always means the frequent regeneration requirement and inevitably results in high operation cost in practice. Therefore, the selective sorption of different ions onto adsorbent material is very important for its further practical use. Saturation capacities of Cs(I), Co(II) and Eu(III) radionuclides onto SnSi were determined experimentally through repeated batch sorption equilibration of 0.05 M of respective chloride salt of each ion.

The study has been extended for the adsorption of ^{134}Cs , ^{60}Co and $^{152+154}\text{Eu}$ in single systems (Individual interactions) on the surface of SnSi (either in Na- or H- form) at constant pH 4, temperature 25 °C and using 0.05 M concentration of each ion salt. Herein, the effect of initial solution pH not studied while pH 4 was chosen in range before the ion hydrolysis. The obtained values of saturation capacity were reported in Table 3. Accordingly, the order of capacity of the metal ions in these aforementioned conditions showed the sequence: $\text{Eu}^{3+} > \text{Co}^{2+} > \text{Cs}^+$. This sequence may be due to the increase of electrostatic interaction of the multivalent cation compared to the monovalent one. On the other hand, the SnSi in case of Na-form showed higher capacity for the studied nuclides than the H-form. Similar trend was reported earlier where the SnSi affinity toward the proton more favorable compared to the other studied ions which is in contrary with the Na^+ in case of Na- form²¹.

Table 3. Ion exchange capacity (meq/g) of ^{134}Cs , ^{60}Co and $^{152+154}\text{Eu}$ radio nuclides on SnSi at $[\text{M}] = 0.05\text{M}$, $\text{V/m} = 100$, pH 4, $\text{T} = 25 \text{ }^\circ\text{C}$

radionuclide	Na-form	H-form
$^{134}\text{Cs}^+$	0.75	0.20
$^{60}\text{Co}^{2+}$	1.24	0.40
$^{152+154}\text{Eu}^{3+}$	2.50	0.81

Effect of temperature and ion selectivity

The efficiency of an ions separation depends on the condition under which selectivity coefficient (K_a) has a useful value, or influencing in a direction favorable to separation. According to the literature, for a given metal ions pair, the electrolyte media in which the separation factor is the highest, is selected as the eluent. Thus, a study on distribution behavior

of metal ions in various electrolyte media gives an idea about the eluents that can be used for separation. In this work, a new separation technique considering the equilibrium temperature effect has been studied. Herein, the distribution coefficients (K_d) of Cs(I), Co(II) and Eu(III) ions onto SnSi at different reaction temperatures were described as shown in Figure 7. The selectivity of SnSi for Eu(III) ions over other metal ions were evaluated from the selectivity coefficient (K_a $\text{Eu}^{3+}/\text{M}^{n+}$). The initial concentration of each metal ion is being kept at 1.0×10^{-4} M and at pH 4. It was observed that with the increase in temperature from 298 to 333 K the % uptake of Co(II) and Eu(III) ions increased from 40 to 72% for Co(II) and from 15 to 37% for Eu(III) at equilibrium which are compatible with the chemisorption mechanism. This increase in adsorption may be either due to acceleration of slow adsorption steps or due to creation of some new active sites³⁶ or due to transport against a concentration gradient, and/or diffusion controlled transport across the energy barrier³⁷. Similar behavior was reported for the adsorption of cerium ions on hydrous ferric oxide³⁸. On contrary, Cs(I) ions revealed decrease in % uptake from 28 to 20% with increasing the temperature from 298 to 333 K. The reduction in sorption efficiency against temperature may be attributed to desorption of physically adsorbed Cs^+ . Similar behavior was reported for the adsorption of Ba^{2+} on TiO_2 powder³⁹. Thus, the uptake of Cs(I) is in accordance with the exothermic adsorption process.

From the view point of separation process and based on this result it can be achieved an improvement in the separation processing of spent fuel containing ^{134}Cs , ^{60}Co and $^{152+154}\text{Eu}$ isotopes from aqueous medium. Regarding the inversely change of K_d with the temperature (Figure 9), binary separation of the ions was determined. Based on this contradictory temperature effect and the concerning mechanism; it can be seen that as the temperature increased from 298 to 333 K, the separation factor (K_a) of $\text{Co}^{2+}/\text{Cs}^+$ binary system increased from 1.72 to 11.55 and for $\text{Co}^{2+}/\text{Eu}^{3+}$ increased from 2.6 to 4.9 and for $\text{Cs}^+/\text{Eu}^{3+}$ increased from 2.27 to 2.3. The distribution ratios and selectivity coefficients with respect to other metal ions using H^+ -SnSi are shown in Figure 9. It can be seen that the distribution ratio of H^+ -SnSi for Eu(III) at 60 °C was 2.0 times greater than that of 25 °C. Based on the results obtained, it is evident that H-SnSi has a strong ability to selectively adsorb certain ion from mixed metal ions in aqueous solution according to the reaction temperature. Accordingly, quantitative binary separation of these metal ions of analytical interest was achieved depending on the temperature change.

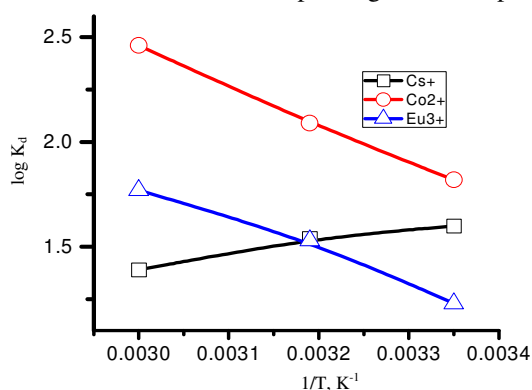


Figure 9. Variation of $\log K_d$ vs. $1/T$ for adsorption of Eu(III), Co(II) and Cs(I) ions on SnSi

Thermodynamic description

Temperature is other important parameter for sorption studies and it tells more about the mechanism involved in the sorption process⁴⁰. Basically, there are two major effects of

temperature on adsorption process. When temperature is increased, the diffusion rate of the adsorbate molecules is increased across the external boundary layer and in the internal pores of the adsorbent particle, due to the decrease in the velocity of the solution⁴¹. In the same vein, variation in the temperature of the adsorption system results into variation in the equilibrium capacity of the adsorbent for a particular adsorbate⁴². Therefore, if the rate of adsorption is increased with temperature, the mechanism controlling the process is endothermic but if the rate is decreased with temperature, it is exothermic. The spontaneity of the process depends on whether the change in entropy and the free energy of adsorption system is positive or negative⁴³. Positive value of entropy change and negative value of free energy change indicate the solution interface is in random increase and spontaneous sorption process, but negative entropy change and positive free energy change show that the solution interface is slow and hence non spontaneous sorption process⁴³. So, it could be said that temperature is responsible for the behavior/nature of sorbate in solution and the availability of active sorption sites on the adsorbent surface as temperature varies⁴⁰. This means that if solution temperature increases, it weakens the electrostatic interactions of the ions in solution and hence, increases their mobility towards sorbent and vice versa. Besides, it is generally known that if sorption is governed by physical phenomenon, an increase in temperature will cause a reduction in sorption capacity. Thermodynamic adsorption investigation plays a key role in estimating adsorptive mechanisms (*i.e.*, physical or chemical)⁴³.

In this work, the dimensionless thermodynamic equilibrium constant (K_c) has been calculated using distribution coefficient constant (K_d)^{44,45}. When the solute concentration approaches zero in the solution, the activity coefficient approaches unity and the thermodynamic equilibrium constant was derived from distribution coefficient constant ($K_d = q_e/C_e$). Milonjić proposed that K_d can be converted into the dimensionless thermodynamic equilibrium constant (K_c) by multiplying K_d by 1000⁴⁶. Based on this approach, parameters like free energy change (ΔG°), enthalpy change (ΔH°) and entropy change (ΔS°) were estimated in the range of 298-333 K under the sorption conditions; 0.05 g SnSi, 5 mL of 1.0×10^{-4} M initial ions concentrations, pH 4, 400 rpm stirring rate and ca. 3 h contact time (Eqs. 12-14). At equilibrium, the standard Gibb's free energy change of the process is related to the distribution coefficient (K_d) by the equation:

$$\Delta G^\circ = -RT \ln K_d \quad (12)$$

The relationship of ΔG° to ΔH° and ΔS° is described as:

$$\Delta G^\circ = \Delta H^\circ - T\Delta S^\circ \quad (13)$$

The well known Van't Hoff equation is obtained by substituting Eq. (12) into Eq. (13)

$$\log K_d = -\Delta H^\circ/2.303RT + \Delta S^\circ/2.303R \quad (14)$$

Where; K_d , R and T are the distribution coefficient (mL/g), universal gas constant (8.314×10^{-3} kJ mol⁻¹ K⁻¹) and adsorption medium absolute temperature (K), respectively.

According to equation (14) the values of ΔH° and ΔS° can be calculated from the slopes ($\Delta H^\circ/2.303R$) and intercepts ($\Delta S^\circ/2.303R$) of $\log K_d$ versus $1/T$ plots as shown in Figure 9^{43,47-49}. The calculated values of thermodynamic parameters were given in Table 4.

As seen from Table 4, for ions sorption on SnSi matrix, ΔH values were found to be -12.75, -15.23 and 5.04 kJ mol⁻¹ for Eu(III), Co(II) and Cs(I) ions, respectively. The values ΔH° are found to be positive for Cs(I) indicating endothermic while it negative for Eu(III) and Co(II) indicating exothermic nature. Although there are no certain criteria related to the ΔH° values that define the adsorption type, these values are frequently assumed as the comparable values for the chemical sorption in case of Eu(III), Co(II) and physical sorption

in case of Cs(I)¹⁵. It is obvious from the obtained ΔH° values that ion exchange mechanism takes place in the adsorption process. The high values of ΔH° were obtained for Eu(III) and Co(II), which is almost confirming to strong bonding with the adsorbent matrix than Cs¹⁵. Negative values of Gibbs free energy (ΔG°), for sorption of Eu(III) and Co(II) ions indicate the spontaneous nature of the reactions. It is possible to say that the adsorptive forces are strong enough to break the potential and shift the reaction ultimately to the right leading to bending of Eu(III) and Co(II) onto surface constituents of SnSi. In addition, the slight increase in negative Gibbs free energy with increasing the reaction temperature means the reaction is favored and getting easier at higher temperatures. Moreover, it could be concluded that the adsorption process of interest was a physisorption process.

Table 4. Values of thermodynamic parameters of Eu³⁺, Co²⁺ and Cs⁺ ion son SnSi

Ions	ΔH° kJ/mole	ΔS° , J/mole K ⁻¹	ΔG° , kJ/mole		
			293	313	333
Eu ³⁺	-12.75	53.12	-28.60	-29.40	-30.40
Co ²⁺	-15.23	66.10	-34.93	-35.92	-37.24
Cs ⁺	5.04	-3.46	15.35	15.86	16.56

Also, the negativity of ΔG° in case of Eu(III) and Co(I) sorption confirms the high preferring with SnSi compared to the protons and vice versa in case of Cs(I)⁵⁰. The values of ΔS° were found to be positive in case of Eu(III) and Co(II) systems while it negative in case of Cs(I). The positivity of ΔS° may be due to the exchange of the ions with more mobile ions present on the exchanger. The positively ΔS° would cause increase in the entropy (increase randomness), during the adsorption process. In this concern, in the case of physic sorption which may also contribute to the total adsorption process can cause increase in entropy. This is because either of the water molecules released from the hydrated ions or the water molecules present on the surface during the adsorption process¹⁵.

Conclusion

The stannic silicate was obtained in a granular character promising or predominant applications. Thermal and XRD analysis indicated that only SnO₂ in cassiterite phase was appeared after heating at 1000 °C. The equilibrium sorption studies of Eu³⁺ revealed that the process obeyed the Freundlich isotherm model while the kinetics of the process indicated the process obeyed the second order kinetic model. Because of both Co(II) and Eu(III) sorption proportionally increase under the effect reaction temperature (exothermic) while Cs⁺ was decreased (endothermic), separation of Eu³⁺, Co²⁺ and Cs⁺ in aqueous solution can be improved.

References

1. Husnain S, Um W, Woojin-Lee and Yoon-Seok Chang, *RSC Adv.*, 2018, **8**, 2521-2540; DOI:10.1039/C7RA12299C
2. Sun Y, Li J and Wang X, *Geochim Cosmochim Acta*, 2014, **140**, 621-643; DOI:10.1016/j.gca.2014.06.001
3. Hurel C, Marmier N and Radioanal J, *Nucl Chem.*, 2010, **284**(1), 225-230; DOI:10.1007/s10967-010-0476-x
4. Lu S, Xu J, Zhang C and Niu Z, *J Radioanal Nucl Chem.*, 2011, **287**(3), 893-898; DOI:10.1007/s10967-010-0849-1

5. Reynolds T, Unit Operation and process in Environmental Engineering, PWS Publishing, NY, USA, 1992.
6. Yang S, Zong P, Ren X, Wang Q and Wang X, *ACS Appl Mater Interface*, 2012, **4**(12), 6891-6900; DOI:10.1021/am3020372
7. Mahmoud M, Rashad G, Metwally E, Saad E and Elewa A, *Appl Clay Sci.*, 2017, **141**, 72-80; DOI:10.1016/j.clay.2016.12.021
8. Hamed M, Holiel M and Ahmed I, *Radiochim Acta*, 2016, **104**(12), 873-890; DOI:10.1515/ract-2016-2579
9. Yang S, Sheng G, Montavon G, Guo Z, Tan X, Grambow B and Wang X, *Geochim Cosmochim Acta*, 2013, **121**, 84-104; DOI:10.1016/j.gca.2013.07.013
10. Sheng G D, Yang S T, Li Y M, Gao X, Huang Y Y, Hu J and Wang X K, *Radiochim Acta*, 2014, **102**(1-2), 155-167; DOI:10.1515/ract-2014-2088
11. Janot N, Benedetti M F and Reille P E, *Environ Sci Technol.*, 2011, **45**(8), 3224-3230; DOI:10.1021/es102592a
12. Dong W, Wang X, Bian X, Wang A, Du J and Tao Z, *Appl Radiat Isot.*, 2001, **54**(4), 603-610; DOI:10.1016/S0969-8043(00)00311-0
13. Naveau A, Monteil-Rivera F, Dumonceau J and Boudesocque S, *J Contam Hydrol.*, 2005, **77**(1-2), 1-16; DOI:10.1016/j.jconhyd.2004.10.002
14. Ali I, Elshorbagy M, Rizk H, El-Sharkawy M and Sadeek S, *J Faculty Sci Zagazig Univ.*, 2016, **38**(2/16), 4187.
15. Ali I, Zakaria E, Shama S and El-Naggar I, *J Radioanal Nucl Chem.*, 2010, **285**(2), 239; DOI:10.1007/s10967-010-0547-z
16. Ali I M, "Synthesis and properties of certain inorganic ion exchange materials for use in the back end of the nuclear fuel cycle" PhD Thesis, Faculty of Science, Mansoura Univ., Dakahlia, Egypt (2000).
17. Oleksienko O, Levchuk I, Sitarz M, Meleshevych S, Strelko V and Mika Sillanpää, *Desalination Water Treatment*, 2016, **57**, 5554-5566; DOI:10.1080/19443994.2014.1003103
18. Rabung T, Stump T, Geckeis H, Klenze R and Kim J I, *Radiochim Acta*, 2000, **88**(9-11), 711-716; DOI:10.1524/ract.2000.88.9-11.711
19. Fan Q, Tan X, Li J, Wang X, Wu W and Montavon G, *Environ Sci Technol.*, 2009, **43**(15), 5776-5782; DOI:10.1021/es901241f
20. Fan Q, Shao D, Lu Y, Wu W and Wang X, *Chem Eng J.*, 2009, **150**(1), 188-195; DOI:10.1016/j.cej.2008.12.024
21. Ali I, Zakaria E and El-Naggar I, *Arab J Nucl Sci Appl.*, 2004, **37**(3), 31.
22. JCPDS-International Centre for Diffraction Data, PCPDFWIN version, 1.30, 1997.
23. Cardoso W, Francisco M, Lucho A and Gushikem Y, *Solid State Ionics*, 2004, **167**(1-2), 165-173; DOI:10.1016/j.ssi.2003.12.017
24. Kurihara L, Fujiwara S, Alfaya R, Gushikem Y, Alfaya A and de Castro S, *J Colloid Interface Science*, 2004, **274**(2), 579-586; DOI:10.1016/j.jcis.2004.01.040
25. Musić S, Vinceković N and Sekovanić L, *Braz J Chem Eng.*, 2011, **28**(1), 89-94; DOI:10.1590/S0104-66322011000100011
26. Galamboš M, Suchánek P and Rosskopfová O, *J Radioanal Nucl Chem.*, 2012, **293**(2), 613-633; DOI:10.1007/s10967-012-1717-y
27. Chen Z, He J, Chen L and Lu S, *J Radioanal Nucl Chem.*, 2016, **307**(2), 1093-1104; DOI:10.1007/s10967-015-4252-9
28. Dolatyari L, Yaftian M and Rostamnia S, *J Taiwan Inst Chem Eng.*, 2016, **60**, 174-184; DOI:10.1016/j.jtice.2015.11.004

29. Duman O, Tunç S and Polat T, *Microporous and Mesoporous Materials*, 2015, 210, DOI:10.1016/j.micromeso.2015.02.040
30. Huang J, Cao Y, Liu Z, Deng Z, Tang F and Wang W, *Chemical Engineering J.*, 2012, **180**, 75-80; DOI:10.1016/j.cej.2011.11.005
31. El-Ashtoukhya E, Amina N and Abdel Wahabb O, *Desalination*, 2008, **223**, 162-173; DOI:10.1016/j.desal.2007.01.206
32. Sparks D, *Soil Physical Chemistry*, 83±145, 1986, CRC Press, Boca Raton, Florida.
33. Clark A, *The theory of adsorption and catalysis*, Academic Press, New York, San Francisco, London p. 210, (1970).
34. Lima J, Ragassi M, Gimenes M, Vieira M and da Silva M, *Chem Engg Trans.*, 2017, **56**; 1891-1896; DOI:10.3303/CET1756316
35. Granados-Correa F, Vilchis-Granados J, Jiménez-Reyes M and Quiroz-Granados L A, *J Chem.*, 2013, DOI:10.1155/2013/751696
36. Gupta R K, Dubey S S and Singh R A, *Sep Purif Technol.*, 2004, **38**(3), 225-232; DOI:10.1016/j.seppur.2003.11.009
37. Mishra S P, Tiwari D, Prasad S K, Dubey R S and Mishra M, *J Radioanal Nucl Chem.*, 2007, **272**(2), 371-379; DOI:10.1007/s10967-007-0531-4
38. Dubey S and Rao B, *J Hazardous Mater.*, 2011, **186**(23), 1028-1032; DOI:10.1016/j.jhazmat.2010.11.085
39. Mishra S P, Srinivasu N and Tiwari D, *Appl Radiat Isot.*, 1992, **43**10, 1253-1257; DOI:10.1016/0883-2889(92)90203-Q
40. Yagub M T, Kanti S T, Sharmeen A and Ang H M, *Adv Colloid Interface Sci.*, 2014, **209**, 172-184; DOI:10.1016/j.cis.2014.04.002
41. Abd El-Rahman K, El-Kamash A, El-Sourougy M and Abdel-Moniem N, *J Radioanal Nucl Chem.*, 2006, **268**(2), 221-230; DOI:10.1007/s10967-006-0157-y
42. Wang S, Boyjoo Y, Choueib A and Zhu Z, *Water Res.*, 2005, **39**(1), 129-138; DOI:10.1016/j.watres.2004.09.011
43. Tran H, Youb S and Chao H, *J Env Chem Engg*, 2016, **4**(3), 2671-2682; DOI:10.1016/j.jece.2016.05.009
44. Khan A and Singh R, *Colloids Surf.*, 1987, **24**(1), 33-42; DOI:10.1016/0166-6622(87)80259-7
45. Nassar M, Ali E and Zakaria E, *RSC Adv.*, 2017, **7**, 8034-8050; DOI:10.1039/C6RA27924D
46. Milonjic S K, *J Serb Chem Soc.*, 2007, **72**(12), 1363-1367; DOI:10.2298/JSC0712363M
47. Granados-Correa F, Vilchis-Granados J, Jiménez-Reyes M and Quiroz-Granados L A, *J Chem.*, 2013, 9; DOI:10.1155/2013/751696
48. Smith J, Van Ness H and Abbott M, *Introd to Chem Eng Thermodynamics*, McGraw Hill, NY, USA, 2005.
49. Ceglowski M and Schroeder G, *Chem Eng J.*, 2015, **263**, 402-411; DOI:10.1016/j.cej.2014.11.047
50. Ali I M, *Chem Eng J.*, 2009, **155**(3), 580-585; DOI:10.1016/j.cej.2009.07.050